Adsorption (2008) 14: 415–422
DOI 10.1007/s10450-007-9100-y

Capture of CO_2 from high humidity flue gas by vacuum swing adsorption with zeolite 13X

Gang Li · Penny Xiao · Paul Webley · Jun Zhang · Ranjeet Singh · Marc Marshall

Received: 30 April 2007 / Revised: 29 September 2007 / Accepted: 27 December 2007 / Published online: 16 January 2008

Abstract Capture of CO_2 from flue gas streams using adsorption processes must deal with the prospect of high humidity streams containing bulk CO_2 as well as other impurities such as SO_x, NO_x, etc. Most studies to date have ignored this aspect of CO_2 capture. In this study, we have experimentally examined the capture of CO_2 from a 12% synthetic flue gas stream at a relative humidity of 95% at 30 °C. A 13X adsorbent was used and the migration of the water and its subsequent impact on capture performance was evaluated. Binary breakthrough of CO_2/water vapor was performed and indicated a significant effect of water on CO_2 adsorption capacity, as expected. Cyclic experiments indicate that the water zone migrates a quarter of the way into the column and stabilizes its position so that CO_2 capture is still possible although decreased. The formation of a water zone creates a "cold spot" which has implications for the system performance. The recovery of CO_2 dropped from 78.5% to 60% when moving from dry to wet flue gas while the productivity dropped by 22%. Although the concentration of water leaving the bed under vacuum was 27%(vol), the low vacuum pressure prevented condensation of water in this stream. However, the vacuum pump acted as a condenser and separator to remove bulk water. An important consequence of the presence of a water zone was to elevate the vacuum level thereby reducing CO_2 working capacity. Thus although there is a detrimental effect of water on CO_2 capture, long term recovery of CO_2 is still possible in a single VSA process. Pre-drying of the flue gas steam is not required. However, careful consideration of the impact of water and accommodation thereof must be made particularly when the feed stream temperature increases resulting in higher feed water concentration.

Keywords CO_2 capture · Pressure swing adsorption · Humid flue gas

Abbreviations

L Length of bed (mm)
P Pressure (kPa)
T Temperature (°C)
Z Dimensionless distance
u Interstitial velocity (mm/s)
t Time (s)
z Axial distance along adsorption bed (mm)
τ Dimensionless time

1 Introduction

Carbon dioxide is the most significant greenhouse gas emitted from human activities and contributes to global warming. As a result there has been wide spread efforts to mitigate and control these emissions. One practical method to reduce carbon dioxide emissions is geo-sequestration which involves capturing carbon dioxide from flue gases and injecting it directly into underground geological formations. VSA (vacuum swing adsorption) is a promising technology for the capture of CO_2 from flue gas streams since it has a number of advantages such as relatively low power consumption and ease of operation.

G. Li · P. Xiao · P. Webley (✉) · J. Zhang · R. Singh
Cooperative Research Centre for Greenhouse Gas Technologies, Department of Chemical Engineering, Monash University, Wellington Road, Clayton, Victoria 3800, Australia
e-mail: paul.webley@eng.monash.edu.au

M. Marshall
School of Chemistry, Monash University, Wellington Road, Clayton, Victoria 3800, Australia

For capture of CO_2 from dry flue gases, simulation studies have shown that CO_2 can be enriched by pressure swing adsorption (PSA) from 17% to 99.997% at a recovery of 68.4% using activated carbon as the adsorbent (Kikkinides et al. 1993) and from 15% to 99% at a recovery of 53% (Chue et al. 1995). Ko et al. (2003) optimized the conditions of the PSA process using zeolite 13X at cyclic steady state (CSS) with a given power constraint. Recently, an experimental study of a three-bed VSA by our group achieved a CO_2 recovery of 90% and purity of 80% from dry flue gas containing 12% CO_2 using zeolite 13X as the adsorbent (Zhang et al. 2005). However, real flue gases include 8–12% CO_2, 8–10% water, and trace amounts of SO_x and NO_x. Even if the flue gas is pre-treated with a wash tower, it will leave saturated with water vapor at concentrations up to 5% at ambient conditions. Since water adsorption on zeolite 13X and many other polar adsorbents is much stronger than CO_2 adsorption, the effect is to displace CO_2 and reduce the adsorbent's capacity for CO_2 capture (Shen and Worek 1994). In the event of high water loading, condensation of water may occur causing high pressure drop and forming corrosive carbonic acid with subsequent corrosion problems. There have been a large number of studies examining the removal of CO_2 and water vapor from gas streams using adsorption processes. However, most of these studies are confined to ppm levels of CO_2 and saturated water vapor for air purification systems (Chang et al. 1991; Rege et al. 2000; Kumar et al. 2003). There are very few reported studies on removing bulk CO_2 in high humidity streams hence the motivation for the current study.

The main objective in this project was to study the feasibility of removing water and CO_2 from wet flue gas streams in a single VSA process, which would have the benefit of lower cost compared with that of a VSA process and a pretreatment drier. It is well known that air separation processes (e.g. O2VSA) accomplish efficient nitrogen/oxygen separation within the same beds which also accomplish water removal, regardless of the humidity of the incoming air stream (Watson et al. 1996).

Initially, we have chosen zeolite 13X (Na exchanged, Si:Al ratio 1.5) as the adsorbent because of its high adsorption capacity for both CO_2 and H_2O under VSA mode. It is also known to be satisfactory for treating air streams during the air separation process. Breakthrough experiments were carried out to study CO_2 and H_2O co-sorption behavior at high levels of CO_2 and water. However, breakthrough data are not sufficient to understand the migration of water during cyclic operation and hence this second aspect was also studied. Cyclic experiments were therefore conducted to investigate the performance of the VSA process for CO_2/H_2O/air and water free CO_2/air feed streams. From our previous work on water adsorption (Wilson et al. 2001), we were able to track the location of the water front during cyclic experiments by using the proxy of the "cold spot" and we report our data on this important aspect of the operation of the CO2VSA process.

2 Experimental work

2.1 Isotherm measurement

The adsorption isotherm data for water vapor on zeolite 13X at 25 °C from P/Po of 0 to 1 was obtained by a gravimetric apparatus (IGA-002 Intelligent Gravimetric Analyzer system manufactured by Hiden Isochema, Ltd. (UK)). The adsorption isotherm data for CO_2 and N_2 on zeolite 13X was obtained by an ASAP 2010 Gas Adsorption Analyzer (Micromeritics, USA) at three temperatures: 20, 40 and 90 °C over the pressure range 0–118 kPa.

2.2 Experimental set-up

A schematic diagram of the laboratory-scale VSA apparatus used in this study is shown in Fig. 1. The main items are a single packed adsorbent bed and a humidifier system. The adsorption bed is made of a stainless steel column with an effective working length of 560 mm, an ID of 49 mm and 3 mm wall thickness. Along the length of the bed ten T type thermocouples were inserted at the position of 60, 100, 140, 180, 220, 260, 300, 387, 474, and 560 mm from the bottom of the bed to measure the temperature profile during the experiment. Thermocouples are also installed at locations in the pipeline to monitor the process fluids entering and leaving the bed. The bed is wrapped with heating tape to maintain the external temperature and nitrile rubber insulation material to reduce heat loss through the column wall.

The humidifier is of the "bubbler" type with a tubular heater placed at the bottom of the tank to control the temperature. Distilled water is injected to the tank and maintained at a certain level. The humidity of the generated wet air is controlled by adjusting the water temperature. The temperature and the relative humidity of the feed gas and effluent gas were analyzed by in situ hydrometers (HMT330, ±0.05% full scale, VAISALA, Finland). The feed line is kept at a slightly elevated temperature with heating tape and insulation material to control the feed gas temperature and prevent water vapor condensation.

The locations of pressure transducers (S902, accuracy $< 1\%$ of reading, MKS), flow meters (EJA115, YokoGawa, Japan), control valves (Type 3510, SAMSON) and carbon dioxide analyzers (Ir1507, intrinsic error $< 0.1\%$ CO_2, Servomex) are also shown in Fig. 1 and are calibrated prior to every experiment. The control, operation and data logging were performed using GeniDAQ® software on a PC.

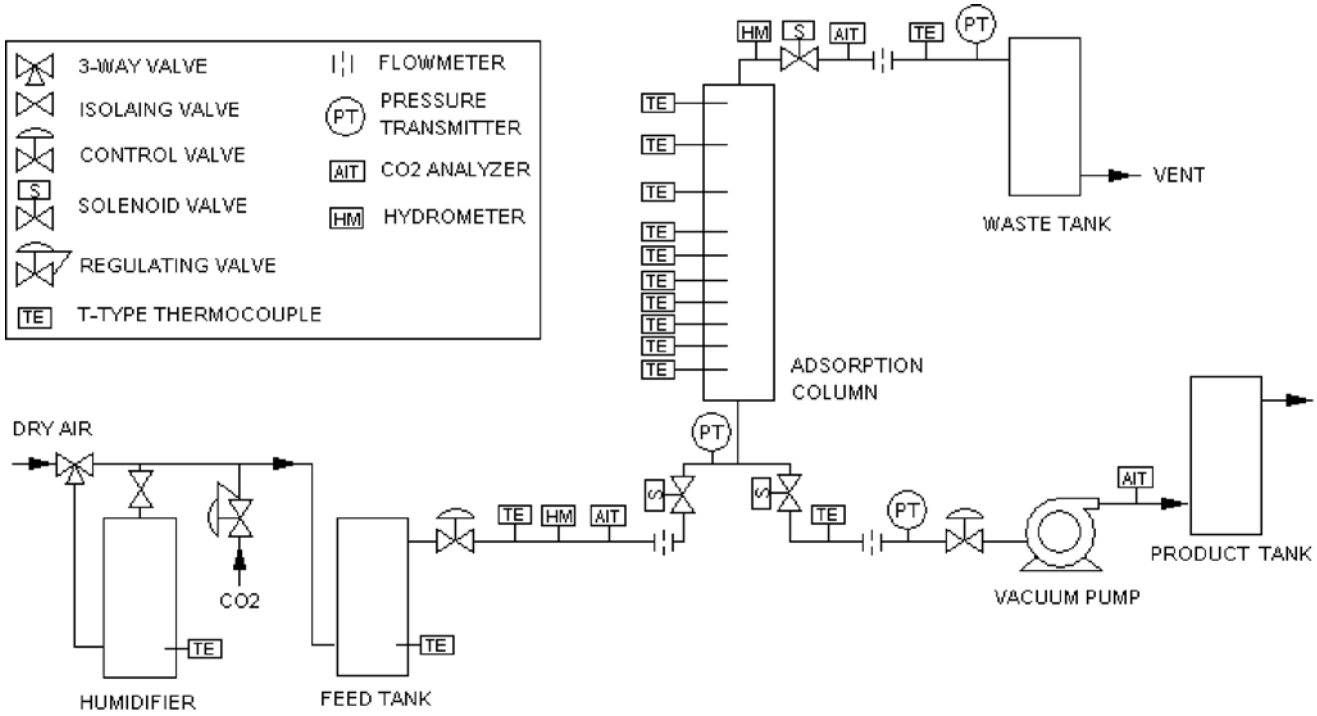

Fig. 1 Process flow diagram for cyclic adsorption experiments

Table 1 Physical properties of zeolite 13X

Property	Zeolite 13X
Chemical description	NaX
Si/Al ratio	1.5
Shape of adsorbent	Spherical
Diameter [mm]	2.0
Bulk density [kg/m^3]	640.7
Total pore vol [cm^3/g]	0.27
Avg pore diam [nm]	2.44
BET surface area [m^2/g]	445.5

The adsorbent selected for this study is zeolite 13X (MOLSIV Adsorbents, UOP LLC) with average bead diameter of 2.0 mm. It was regenerated at 320 °C before using. The physical properties of zeolite 13X are included in Table 1.

2.3 VSA cycle

A simple three-step VSA cycle was used in this study (Fig. 2) with the objective of studying the migration of the water front, establishing the feasibility of removing large quantities of water from a humid flue gas stream, and examining the impact on the CO_2 capture performance. We emphasize that this is not a cycle one would use in commercial CO_2 capture plants since the latter would involve additional

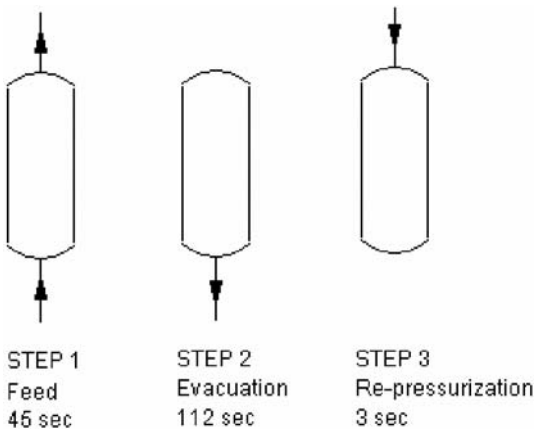

Fig. 2 Three-step VSA cycle

steps such as pressure equalization, product purge, etc. The steps are:

Step 1: Adsorption with feed gas. The feed gas passes through the adsorption bed from bottom to top. This step is fixed at 45 s. This is based on the given flow rates possible with our valving and piping system, the size of the beds and the need to utilize the maximum bed length for CO_2 adsorption without breakthrough.

Step 2: Countercurrent evacuation. The adsorbed components are removed counter-currently into the vacuum line by the vacuum pump. The bed is regenerated and this step is 112 s. This is based on a compromise between cycle

Table 2 Experimental conditions

Experiment	Feed composition (vol%)	Pressure (kPa)	Temperature (°C)	Flowrate (litre/min)
CO_2 breakthrough	CO_2 9.2; air 90.8	120	30	60
H_2O breakthrough	H_2O 3.5; air 96.5	114	30	52.5
Wet CO_2 breakthrough	CO_2 8.8; H_2O 3.4; air 87.8	115	30	46
CO_2 VSA	CO_2 11.2; air 88.8	119	30	71
Wet CO_2 VSA	CO_2 12; H_2O 3.4; air 84.6	118	30	63

scheduling constraints as well as reasonable kinetics of desorption and vacuum pump capacity.

Step 3: Re-pressurization with waste. The bed is re-pressurized to atmospheric pressure with waste gas from the top of the bed. This step is 3 s.

2.4 Experimental procedure

Breakthrough and cyclic VSA experiments of CO_2/air or CO_2/H_2O/air binary were conducted according to the conditions summarized in Table 2. To compare data on a uniform basis, the axial distance and time were nondimensionalized as:

$$Z = \frac{z}{L}, \qquad \tau = \frac{ut}{L}.$$

The criteria used to characterize the VSA performance included (amongst others):

Water to carbon dioxide ratio:

$$H_2O/CO_2 = \frac{H_2O \text{ vapor concentration}}{CO_2 \text{ concentration}}. \tag{1}$$

CO_2 and H_2O recovery:

$$\text{Recovery}_{CO_2} = \frac{(\text{Amount of } CO_2 \text{ in feed} - \text{amount of } CO_2 \text{ in waste}) \times 100}{\text{Amount of } CO_2 \text{ in feed}}, \tag{2}$$

$$\text{Recovery}_{H_2O} = \frac{(\text{Amount of } H_2O \text{ in feed} - \text{amount of } H_2O \text{ in waste}) \times 100}{\text{Amount of } H_2O \text{ in feed}}, \tag{3}$$

CO_2 productivity:

$$\text{Productivity} = \frac{\text{Amount of } CO_2 \text{ recovered per hour}}{\text{Amount of adsorbent}}. \tag{4}$$

3 Result and discussion

3.1 Equilibrium isotherm

As shown in Fig. 3(a), the equilibrium isotherm of water on zeolite 13X is highly favorable in the low relative humidity (RH) range with a substantial increase of loading. At high RH ranges (> 55%), capillary condensation is a dominant adsorption mechanism (Ahn and Lee 2004; Lee et al. 2002). The water isotherm is of Type II and still retains a substantial working capacity under VSA conditions. Figure 3(b) shows the CO_2 and N_2 isotherms on 13X with

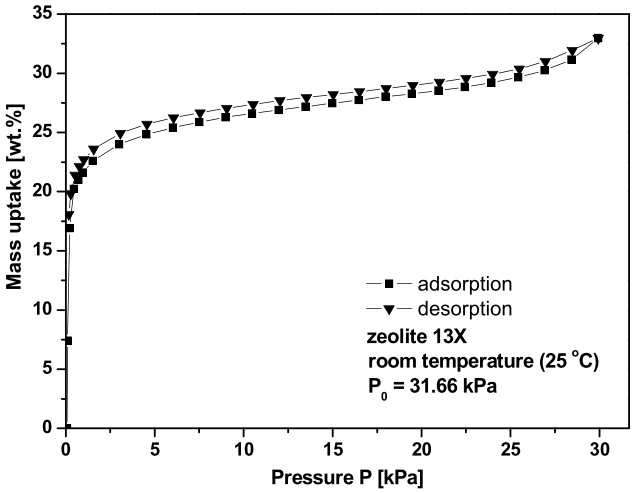

(a)

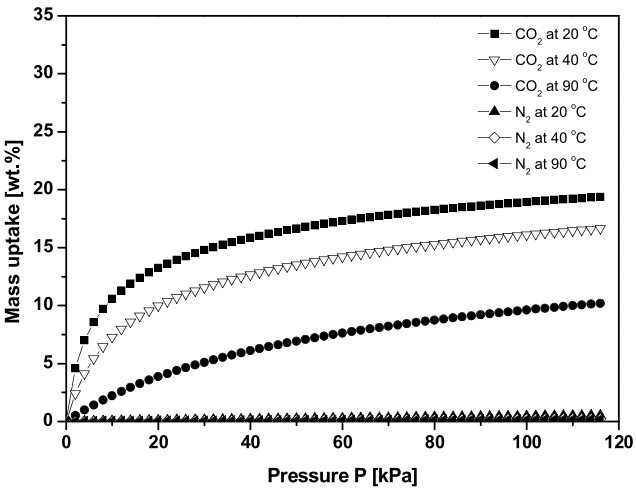

(b)

Fig. 3 (**a**) Isotherm data of water vapor, (**b**) CO_2 and N_2 on zeolite 13X

the well known high selectivity of 13X for CO_2 over N_2 evident. It should also be noted that water adsorption onto 13X is substantially larger than that of CO_2 with a much larger heat of adsorption (the heat of adsorption of CO_2 on 13X is 34.44 kJ, and H_2O on 13X is 51.66 kJ, Rege et al. 2001). We do not currently have binary equilibrium data for the CO_2/water system although preliminary data on our TGA system suggests water adsorption on 13X does not exclude CO_2 altogether.

3.2 Breakthrough analysis

The breakthrough curves of CO_2/H_2O + air were compared with that of CO_2 + air and H_2O + air, as presented in Fig. 4(a). It is clear from Fig. 4(a) that the weaker adsorbing component CO_2 proceeds faster in the column than the stronger component H_2O. The breakthrough of water has a sharp front due to the highly favorable adsorption at low humidity but a proportionate effect was also observed because of capillary adsorption at high humidity (Ahn and Lee 2004). As the front of water propagates in the column, the weaker component CO_2 will be displaced and pushed to the end of the column. Consequently the outlet CO_2 concentration will be much higher than the inlet one thus causing the roll-up effect (Carter and Husain 1974; Shen and Worek 1994; Mellow and Eić 2002). In this paper a very profound roll-up occurred quickly following the CO_2 front and it is likely to be enhanced by the large thermal wave (ΔT up to 100 °C) produced by H_2O adsorption (not shown).

As shown in Fig. 4(a), the equilibrium capacity of water vapor on zeolite 13X was reduced by 14% in the case of CO_2/H_2O + air, as a result of competitive co-adsorption with CO_2, while the capacity of CO_2 decreased by 99% in the presence of H_2O. It appears that the stronger component H_2O adsorption capacity was slightly influenced by weaker component CO_2, whereas the adsorption of CO_2 was dramatically inhibited by H_2O.

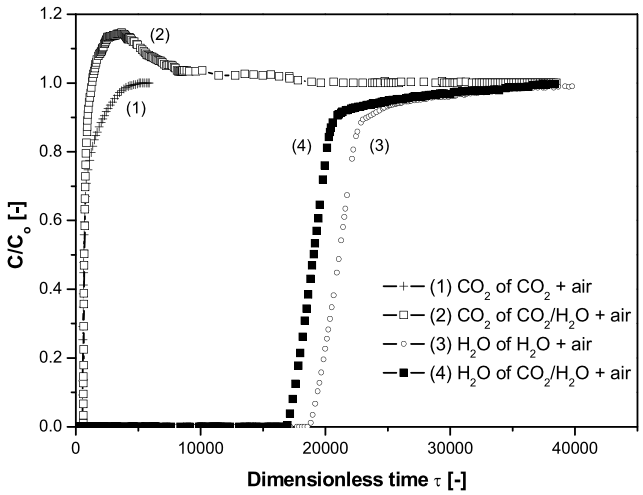

(a)

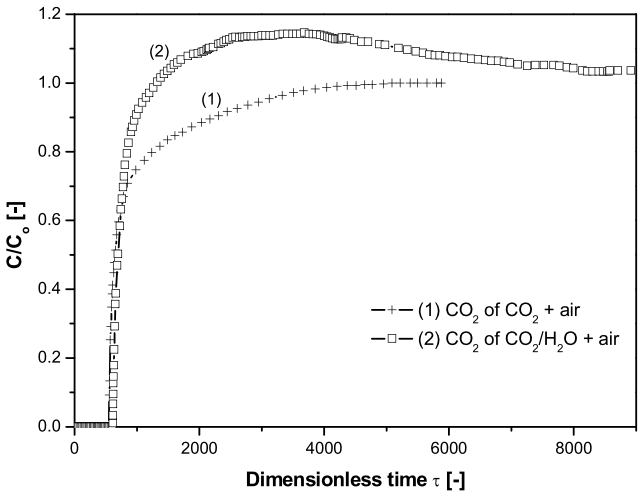

(b)

Fig. 4 (**a**) Breakthrough curves for CO_2 + air, H_2O + air, and CO_2/H_2O + air in zeolite 13X column at 30 °C. (**b**) Magnified image for the CO_2 breakthrough

3.3 Cyclic experiments—dry CO_2 feed gas

Cyclic vacuum swing experiments with dry feed (pre-dried) were carried out at room temperature for comparison with the case of humidified CO_2 feed. Temperature profiles of the column at the end of the feed and evacuation step, respectively, in a cycle at CSS are shown in Fig. 5. The bottom and middle of the bed had a pronounced temperature change up to 16 °C from adsorption to desorption where CO_2 was mainly adsorbed and desorbed, while at the top of the bed the temperature swing is smaller since the adsorption front

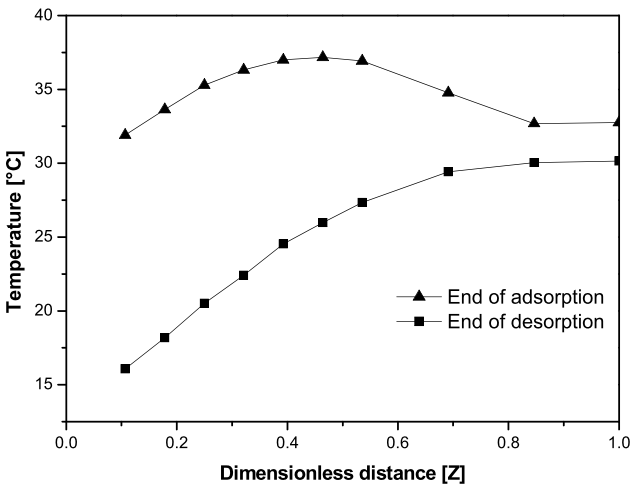

Fig. 5 Axial temperature profiles at the end of the feed step and at the end of evacuation step in different cycles at CSS for dry CO_2 feed at 30 °C

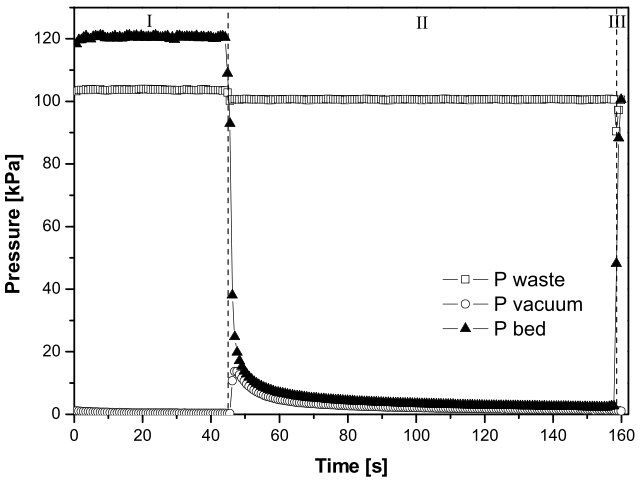

Fig. 6 Pressure profile along a complete cycle at CSS in the case of dry CO_2 VSA. (*I*) Adsorption step; (*II*) Desorption step; (*III*) Re-pressurization step

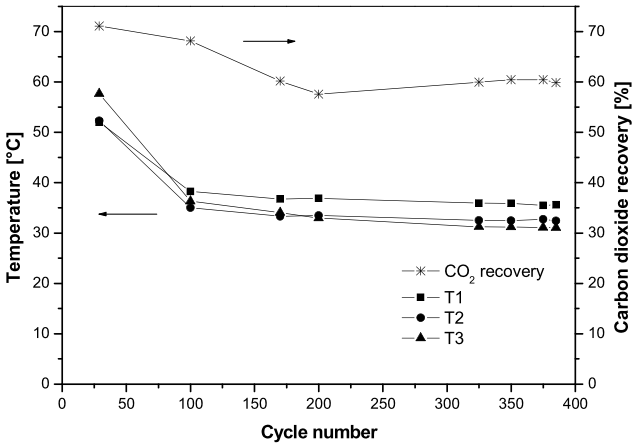

Fig. 7 Evolution of the cold spot at the end of adsorption step and the evolution of carbon dioxide recovery

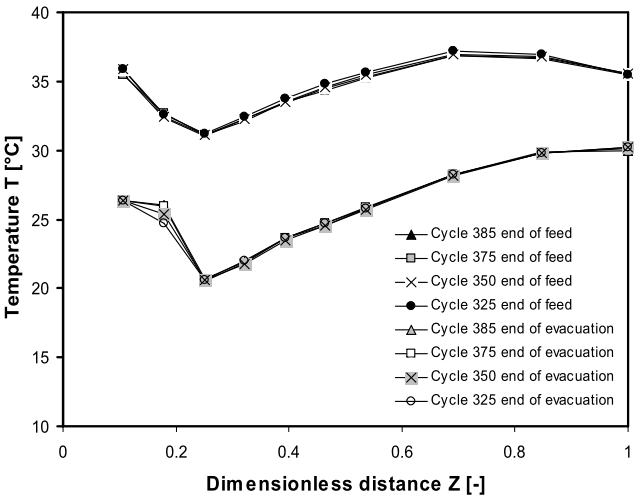

Fig. 8 Axial temperature profiles at the end of the feed step and at the end of the evacuation step in different cycles at CSS for humidified CO_2 feed at 30 °C

is partially contained in order to provide a reasonable CO_2 recovery. The pressure profile in a complete cycle under CSS operation is presented in Fig. 6. which shows that the vacuum pressure reduces rapidly to 3 kPa during the desorption step. Experiments with the dry CO_2 feed gas produced a recovery of 78.5%, a CO_2 purity of 69% and a productivity of 0.287 kg/hr/kg.

3.4 Cyclic experiments—humidified CO_2 feed gas

In the case of a humidified feed gas, the mass transfer front of the faster moving component CO_2 will reach the top of the bed while the slower moving water front is expected to occupy a much smaller adsorption zone near the base of the bed. A water loaded zone will substantially change the temperature profile and performance of the bed and thus create a de facto multilayered bed. The boundary between the wet and dry layers is always associated with the "cold spot" that is an axial temperature depression occurring in layered VSA/PSA. The cold spot results from the interaction between convective heat transfer and heating and cooling by adsorption which has been studied extensively in oxygen VSA (Wilson et al. 2001). A layered bed (either actual layered bed or a *de facto* layered bed) with differing adsorption capacities and thermal behavior is the prerequisite for the formation of the cold spot in the boundary between the layer. While this may be detrimental to the performance of the process, the "cold spot" also acts as a useful diagnostic to track the location of the water front, as discussed below.

The axial temperature evolution was observed along the entire bed. For brevity we show the profiles at the bottom of the bed only in Fig. 7—these are given by thermocouples T1, T2 and T3 (at $Z = 60$, 140 and 220 mm from the feed). In the first tens of cycles, T1 was found to be the lowest temperature, but the evolution of the thermal profile and resultant movement of the cold spot (cooling down quickly from 52.5 °C to 35 °C at cycle 100, and then slowly to 34 °C at cycle 170) meant that eventually the depression reached T3 at cycle 190 and gradually reached steady state at 31 °C after 300 cycles. As the water front slowly approaches the cyclic steady state position, there is no net heating or cooling and the energy is balanced throughout the water zone and indeed the entire column (Wilson et al. 2001). Figure 8 shows the final axial profile in the column and the cold spot is evident. In addition, the temperature swing from adsorption to desorption is now around 10 °C much reduced from its value of 16 °C for the case of dry CO_2 feed.

3.5 Evolution of the water loaded zone

Since the cold spot reflects the position of the boundary layer i.e. water front, one may infer the evolution of the water

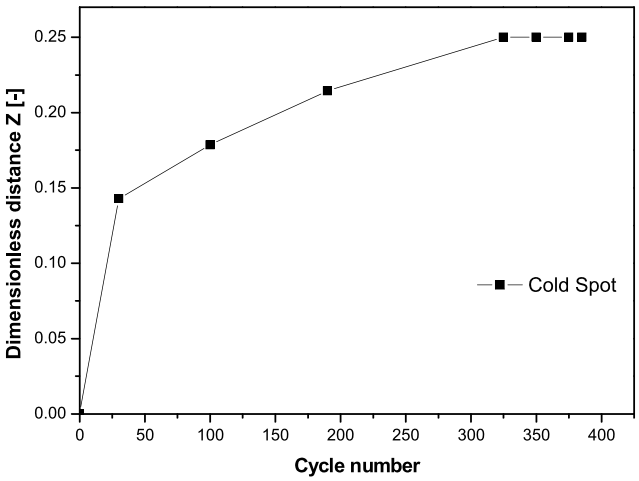

Fig. 9 The evolution of the water front according to the position of the cold spot

loaded zone by plotting the position of cold spot with cycle number (Fig. 9). The position of the cold spot was considered in the middle of two thermocouple positions at the transition state, for example, when T1 ($Z = 0.107$) and T2 ($Z = 0.179$) read the same temperature at cycle 33, the cold spot was taken as at $Z = 0.143$. We note that approximately 300 cycles are needed to stabilize the position of the thermal profiles.

3.6 Performance of VSA with humidified CO_2 feed gas

Operation with the humidified CO_2 stream gave a CO_2 recovery = 60.4% and H_2O recovery = 100% at CSS. The evolution of CO_2 recovery is shown in Fig. 7 and closely tracks the movement of the water front decreasing from 71% to 60%. This is due to the reduction in effective bed length as the water zone progresses. The water front stabilizes at a location at which point the amount of water entering the column equals the water removed by evacuation at CSS. It should be noticed that there was no trace of water detected in the waste stream from the top of the bed throughout the experiment. For this single bed three step VSA operation at CSS, a purity of 72% and a productivity of 0.225 kg/hr/kg was achieved, a reduction in productivity of 22% from the dry gas value. While some of this reduction is due to the loss of available bed due to water, it should also be noted that the ultimate vacuum level reached for the wet CO_2 feed stream was 4 kPa, an increase of pressure of 1 kPa beyond its value for dry CO_2. This will also impact on the recovery and productivity of CO_2. It is apparent that the co-adsorption of water and slow desorption has resulted in an elevated vacuum level. Even prolonged evacuation times were not successful in lowering the vacuum pressure. It should be noted that we have not altered the process conditions to suit the wet feed gas—it is likely that the reduction in productivity can be offset somewhat by a change in process conditions.

3.7 Effect of condensed water

It is known that condensed water may cause large pressure drop and form corrosive carbonic acid with carbon dioxide. It is important therefore to establish the likelihood of water vapor condensation in the adsorbent bed during cyclic operation. The feed stream contained 3.4% H_2O at 30 °C and 118 kPa, giving a relative humidity of 95% hence the water vapor does not condense in the adsorption step. The gas stream leaving the bed in the vacuum line has 27% water vapor at a vacuum pressure of 4 kPa (at the end of evacuation) and thus the water partial pressure is below its saturation pressure at 20 °C and does not condense in the bed or the vacuum line. However, the CO_2 product gas contained only 2.3% water vapor at room temperature indicating that the water had condensed in the vacuum pump when the pressure rose from the suction to the exhaust. Indeed, operation of the vacuum pump was restricted to 4 hours to remove condensed water. This has important implications for continuous operation of large scale CO_2 capture plants. A suitable choice of liquid ring vacuum pump may accommodate condensation and removal of water from the vacuum stream.

4 Conclusions

In this study we experimentally examined the capture of CO_2 in a vacuum swing process in the presence of high humidity. Several observations are of interest. Water can be successfully removed in the same 13X adsorbent bed as the CO_2 stream. The water front stabilizes in the bed at a dimensionless position of 0.25 (140 mm). The presence of the water zone impacts the CO_2 capture in several ways. Firstly, the formation of the water zone creates a *de facto* multilayer resulting in thermal regeneration and a "cold spot". This changes the thermal profiles in the bed and hence the system performance. Secondly, the presence of a water saturated zone and its subsequent slow desorption during evacuation results in a vacuum level which is elevated above its value for dry CO_2 feed. The impact is to reduce CO_2 recovery, purity and productivity. Thirdly, the high water level (27%) in the vacuum stream does not condense in the vacuum line but is collected in the vacuum pump and subsequently recovered.

References

Ahn, H., Lee, C.-H.: Effects of capillary condensation on adsorption and thermal desorption dynamics of water in zeolite 13X and layered beds. Chem. Eng. Sci. **59**, 2727–2743 (2004)

Carter, J.W., Husain, H.: The simultaneous adsorption of carbon dioxide and water vapor by fixed beds of molecular sieves. Chem. Eng. Sci. **29**, 267–273 (1974)

Chang, C.H., Stonesifer, G.T., Cusick, R.J., Hart, J.M.: Comparison of metal oxide absorbents for regenerative carbon dioxide and water vapor removal for advanced portable life support systems. In: 21st International Conference on Environmental Systems, San Francisco, pp. 1–10 (1991)

Chue, K.T., Kim, J.N., Yoo, Y.J., Cho, S.H., Yang, R.T.: Comparison of activated carbon and zeolite 13X for CO_2 recovery from flue gas by pressure swing adsorption. Ind. Eng. Chem. Res. **34**, 591–598 (1995)

Kikkinides, E.S., Yang, R.T., Cho, S.H.: Concentration and recovery of CO_2 from flue gas by pressure swing adsorption. Ind. Eng. Chem. Res. **32**, 2714–2720 (1993)

Ko, D., Siriwardane, R., Biegler, L.T.: Optimization of a pressure-swing adsorption process using zeolite 13X for CO_2 sequestration. Ind. Eng. Chem. Res. **42**, 339–348 (2003)

Kumar, R., Huggahalli, M., Deng, S., Andrecovich, M.: Trace impurity removal from air. Adsorption **9**, 243–250 (2003)

Lee, J.S., Kim, J.H., Kim, J.T., Suh, J.K., Lee, J.M., Lee, C.H.: Adsorption equilibria of CO_2 on zeolite 13X and zeolite X/Activated carbon composite. J. Chem. Eng. Data **47**, 1237–1242 (2002)

Mellow, M., Eić, M.: Adsorption of sulfur dioxide from pseudo binary mixtures on hydrophobic zeolites: modeling of the breakthrough curves. Adsorption **8**, 279–289 (2002)

Rege, S.U., Yang, R.T., Buzanowski, M.A.: Sorbents for air prepurification in air separation. Chem. Eng. Sci. **55**, 4827–4838 (2000)

Rege, S.U., Yang, R.T., Qian, K., Buzanowski, M.A.: Air-prepurification by pressure swing adsorption using single/layered beds. Chem. Eng. Sci. **56**, 2745–2759 (2001)

Shen, C.M., Worek, W.M.: Cosorption characteristics of solid adsorbents. J. Heat Mass Transf. **37**, 2123–2129 (1994)

Watson, C.F., Whitley, R.D., Meyer, M.L.: Multiple zeolite adsorbent layers in oxygen separation. U.S. Patent, US005529610A, to Air Products and Chemicals, Inc. (1996)

Wilson, S.J., Beh, C.C.K., Webley, P.A., Todd, R.S.: The effects of a readily adsorbed trace component (water) in a bulk separation PSA process: the case of oxygen VSA. Ind. Eng. Chem. Res. **40**, 2702–2713 (2001)

Zhang, J., Webley, P., Xiao, P.: Experimental pilot-scale study of carbon dioxide recovery from flue gas streams by vacuum swing adsorption. In: AIChE 2005 Annual Meeting, Cincinnati (2005)